Back-EMF ZCP Error Induced by Electromagnetic Structure of Spindle Motor

C. Bi, N. P. Hla, Q. Jiang, and C. S. Soh

Data Storage Institute, A*Star, Singapore 117608

In a hard disk drive (HDD), the zero crossing points (ZCPs) of back-EMF generated in the spindle motor armature windings are used as rotor position signal for realizing precision motor speed control. The error of ZCP is a major concern, especially for HDDs with ultrahigh data recording densities. In the paper, several causes that induce the ZCP error are analyzed, and these problems are induced during the motor design and production. Both the analytical and numerical methods are used in the analysis to study the influence of the electromagnetic structure on the ZCP. Solutions are then proposed to reduce the errors of the ZCP during the motor design phase.

***Index Terms*—Back-EMF, data recording, magnetic motive force, permanent magnet, speed control, speed error, synchronous motor drives, winding.**

I. Introduction

INCREASING the data recording density is of great importance in the hard disk drive (HDD) industry. When the areal data density is further increased, the speed accuracy of the spindle motor is critical to the HDD as the speed error causes the signal-to-noise ratio (SNR) of the data signal to worsen in data reading.

Now all the spindle motor in HDDs are driven by sensorless drive mode, e.g., sensorless BLDC drive mode. Fig. 1 shows the power bridge circuit of the drive system. Using the BLDC drive mode, one electric drive cycle is formed by 6 steps, and in each, the back-EMF of the windings can be detected in its silent intervals; see Fig. 2.

In normal operation, the back-EMF changes from positive value to negative value, or vice versa. Therefore, zero crossing points (ZCPs) of back-EMF happen in the silent intervals. For the three-phase motor with p magnetic pole-pairs, there are 6 p ZCPs in one rotor revolution. These ZCPs are determined by the motor electromagnetic (EM) structure, and they are fixed when the motor has been made. For a perfect motor operating at constant speed, the ZCPs are distributed equivalently in space. Therefore, it is logical to use these ZCPs to detect the rotor position for determining drive current commutation, and calculate the motor speed with the following equation:

$$\Omega_n = \frac{\Delta\theta_n}{\Delta t_n} = \frac{\theta_{zcp(n)} - \theta_{zcp(n-1)}}{t_{zcp(n)} - t_{zcp(n-1)}} \tag{1}$$

where $\theta_{\mathrm{zcp(n)}}$ is the position where the nth ZCP appears, and $\mathrm{t_{zcp(n)}}$ is the time when the nth ZCP appears.

In ideal state, the ZCP interval $\Delta\theta_{\mathrm{n}}$ is always 60 electric degrees. Therefore, from the variation of $\Delta \mathrm{t_n}$, the motor speed at time $\mathrm{t_{zcp(n)}}$ can be known through the numerical differential described by (1). However, the equation shows also that, the speed obtained with (1) is sensitive to the ZCP jitter, i.e., the error of ZCP signal. Reducing the error to minimum level is necessary.

It will be explained later, the ZCP contains always error between each ZCP pairs in the motor operation. However, the accumulation error of ZCP in one revolution can be considered as zero. For weakening the influence of the error to the motor speed detection, the following equation is thus used to calculate the speed

$$\Omega_n = \frac{\theta_{zcp(n)} - \theta_{zcp(n-6p)}}{t_{zcp(n)} - t_{zcp(n-6p)}}. \tag{2}$$

It is clear, using (2) to calculate the speed, the one obtained is the average of the speed in the past 360° rotation. Even if

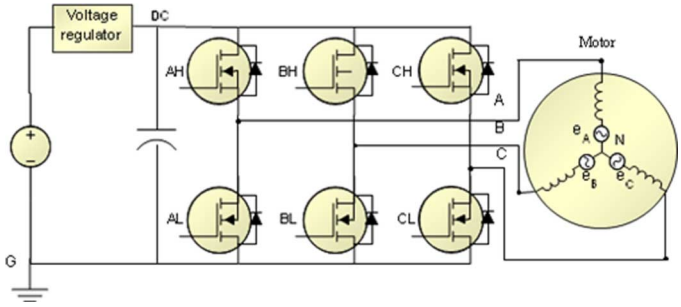

Fig. 1. Power bridge circuit for BLDC drive.

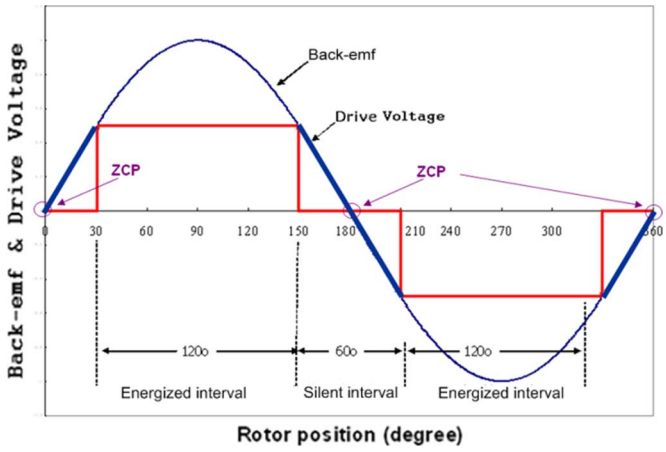

Fig. 2. ZCP generated in spindle motor driving.

Manuscript received December 14, 2010; revised March 11, 2011; accepted March 15, 2011. Dte of current version June 24, 2011. Corresponding author: N. P. Hla (e-mail: Hla_nu_phyu@dsi.a-star.edu.sg).

Color versions of one or more of the figures in this paper are available online at http://ieeexplore.ieee.org.

Digital Object Identifier 10.1109/TMAG.2011.2157895

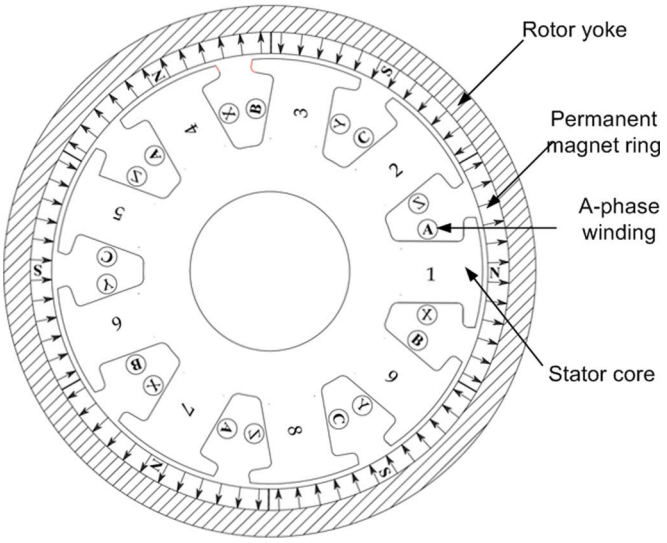

Fig. 3. M1: A spindle motor with 3-pole-pairs and 9 stator slots.

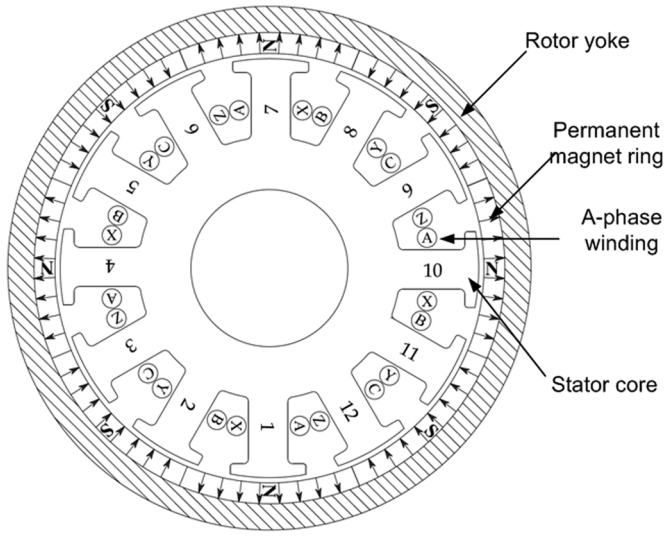

Fig. 4. M2: A spindle motor with 4-pole-pairs and 12 stator slots.

using such a method to detect the motor speed, the position error between one pair of ZCP can still affect the accuracy of speed detection.

For a real spindle motor, as the problems in the motor component quality and motor production, $\Delta\theta_{\rm n}$ contains error, i.e., $\Delta\theta_{\rm n}$ is not constant even if the motor speed is constant. Therefore, even if the $t_{\rm zcp(n)}$ can be detected accurately, the motor speed cannot be detected precisely in using (1). For developing the HDD with ultrahigh data recording density, the influences inducing the ZCP errors should be investigated, and the solution to improve the ZCP accuracy must be developed.

II. The Pole-Pitch Error of the Permanent Magnet and Its Influence to ZCP

The back-EMF generated in the armature winding of the motor is induced by the variation of the flux-linkage in the winding

$$e_k(t) = -\frac{d\Psi_k(t)}{dt} \tag{3}$$

where $e_k(t)$ and $\psi_k(t)$ are the back-EMF and flux-linkage in the kth phase winding, separately. For a three-phase motor, k can be a, b, or c. If the speed operates in constant speed ω, the equation in the time domain can be changed to the one in space domain

$$e_k(\theta) = -\frac{d\Psi_k(\theta)}{d\theta}\cdot\frac{d\theta}{dt} = -\omega\frac{d\Psi_k(\theta)}{d\theta}. \tag{4}$$

As the requirements in the speed control and motor starting, multiple magnetic pole-pair electromagnetic (EM) structure is used in the spindle motor [1]. Fig. 3 shows the EM structure of a spindle motor with 3 magnetic pole-pair and 9 stator slot/teeth, and Fig. 4 shows the one with 4 magnetic pole-pair and 12 stator slot/teeth. They will be called M1 and M2 separately in the paper. For these two motors, every 3 stator slots form one (3S/1p), or two (3S/2p), electrical cycle, to match the magnetic pole-pair of the permanent magnet (PM) ring on the rotor.

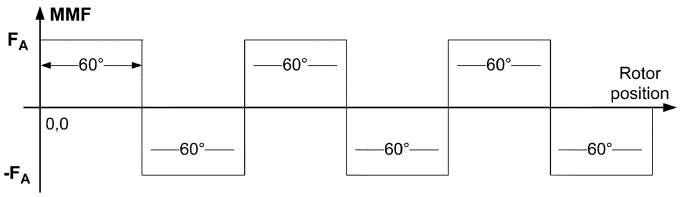

Fig. 5. The MMF of the PM ring in M1, where, the pole-pitches are accurate.

For a motor with p magnetic pole-pair, the flux linkage of one phase winding is the sum of the flux-linkage under different pole-pair, i.e.,

$$\Psi_k(\theta) = \sum_{i=1}^{p}\Psi_k^{(i)}(\theta) \tag{5}$$

where $\psi_k^{(i)}$ is the flux-linkage contributed by the ith pole-pair of the PM ring, and p is the magnetic pole-pail of the motor.

For simplifying the analysis, the airgap magnetic field contributed by the PM ring can be described by using the magnetic-motive-force (MMF). For a perfect PM ring, its MMF waveform in the space domain is cyclic symmetric in space, i.e., the pole-pitch between any consecutive poles of the PM ring is 180 electric degree. Fig. 5 shows the MMF of the PM ring in M1.

The MMF generated by the magnet, $\rm F_m$, shown in Fig. 5 can be expressed with Fourier series

$$F_m(p\theta) = \sum_{n=1} f_n Sin\left[(2n-1)p\theta\right] \tag{6}$$

where $\rm f_n$ is the amplitude of the nth MMF harmonic, and it is determined by

$$f_n = \frac{p}{\pi}\int_0^{\pi/p} F_A Sin\left[(2n-1)p\theta\right]d\theta = \frac{2F_A}{(2n-1)\pi}. \tag{7}$$

When $\mathrm{F_m}$ is known, it is not difficult to know the magnetic flux density, $\mathrm{B}(\theta)$, in the airgap

$$B(\theta) = c_m F_m(\theta) \tag{8}$$

where $\mathrm{c_m}$ is a constant determined by motor airgap length, thickness of the magnet, and the magnetic material used in the PM ring.

For the motor operates with speed ω, the flux generated in one pole range is

$$\begin{aligned}\phi(\omega t) &= \int_{\omega t}^{2\pi/(3p)+\omega t} B(\theta)d\theta = c_m \int_{\omega t}^{2\pi/(3p)+\omega t} F_m(\theta)d\theta \\ &= c_m \int_{\omega t}^{2\pi/(3p)+\omega t} \sum_{n=1} f_n \mathrm{Sin}\left[(2n-1)p\theta\right]d\theta \\ &= -\frac{c_m}{p}\sum_{n=1}\frac{f_n\left\{\mathrm{Cos}\left[(2n-1)p\omega t\right]-\mathrm{Cos}\left[\frac{(2n-1)(2\pi+3p\omega t)}{3}\right]\right\}}{2n-1}.\end{aligned} \tag{9}$$

The back-EMF of the phase winding can thus be calculated as

$$\begin{aligned}e(\omega t) &= -pw\frac{d\phi}{dt} \\ &= pw\omega c_m \sum_{n=1} f_n \left\{\mathrm{Sin}\left[(2n-1)p\omega t\right]\right. \\ &\qquad \left. -\mathrm{Sin}\left[\frac{(2n-1)(2\pi+3p\omega t)}{3}\right]\right\} \\ &= pw\omega c_m \left[F_m(p\omega t) - F_m(p\omega t + 2\pi/3)\right]\end{aligned} \tag{10}$$

where w is the winding turns around one stator tooth. Therefore, the ZCP distribution of back-EMF can be known from the distribution of $F_m(p\theta)$.

However, in magnetizing the PM ring, the pole-pitch cannot be controlled accurately. One reason is that, there are certainly dimension tolerances in the charging model; and another reason is, model deformation is induced in the magnetization procedure [3]–[5].

If the pole-pitch is not accurate, $F_m(p\theta)$ contains more harmonics, and it can be expressed as

$$F_m(p\theta) = F_{ms}(p\theta) + F_{mc}(p\theta) \tag{11}$$

where

$$F_{ms}(\theta) = \sum_{n=1}\left\{f_{ns}\mathrm{Sin}[n\theta]\right\} \tag{12}$$

and

$$F_{mc}(\theta) = \sum_{n=1}\left\{f_{nc}\mathrm{Cos}[n\theta]\right\}. \tag{13}$$

For the MMF harmonic whose order is not the multiple of p, the magnetic pole-pair, the related field cannot induce back-EMF in the winding, and shouldn't be considered in this paper. Equations (12) and (13) can thus be rewritten as

$$F_{ms}(p\theta) = \sum_{n=1}\left\{f_{ns}\mathrm{Sin}[np\theta]\right\} \tag{14}$$

and

$$F_{mc}(\theta) = \sum_{n=1}\left\{f_{nc}\mathrm{Cos}[np\theta]\right\}. \tag{15}$$

Compared with the case with symmetric MMF described by (6) the pole-pitch errors induces the MMF harmonics with even n, and also the additional items described by (15). The coefficients in (14) and (15) can be expressed as the ones shown in (16) and (17)

$$\begin{aligned}f_{ns} &= \frac{1}{\pi}\sum_{k=1}^{p}\left[\int_{\frac{(2k-2)\pi}{p}+\alpha_{2k-2}}^{\frac{(2k-1)\pi}{p}+\alpha_{2k-1}} F_P\mathrm{Sin}(np\theta)d\theta\right. \\ &\qquad \left. -\int_{\frac{(2k-1)\pi}{p}+\alpha_{2k-1}}^{\frac{2k\pi}{p}+\alpha_{2k}} F_N\mathrm{Sin}(np\theta)d\theta\right] \\ &= \frac{F_P}{np\pi}\sum_{k=1}^{p}\left\{\mathrm{Cos}(np\alpha_{2k-2}) - \mathrm{Cos}\left[n(\pi - p\alpha_{2k-1})\right]\right\} \\ &\quad + \frac{F_N}{np\pi}\sum_{k=1}^{p}\left\{\mathrm{Cos}(np\alpha_{2k}) - \mathrm{Cos}\left[n(\pi - p\alpha_{2k-1})\right]\right\}\end{aligned} \tag{16}$$

$$\begin{aligned}f_{nc} &= \frac{1}{\pi}\sum_{k=1}^{p}\left[\int_{\frac{(2k-2)\pi}{p}+\alpha_{2k-2}}^{\frac{(2k-1)\pi}{p}+\alpha_{2k-1}} F_P\mathrm{Cos}(np\theta)d\theta\right. \\ &\qquad \left. -\int_{\frac{(2k-1)\pi}{p}+\alpha_{k-1}}^{\frac{2k\pi}{p}+\alpha_{2k}} F_N\mathrm{Cos}(np\theta)d\theta\right] \\ &= \frac{F_P}{np\pi}\sum_{k=1}^{p}\left[\mathrm{Sin}\left[n(p\alpha_{2k-1} - \pi)\right] - \mathrm{Sin}(np\alpha_{2k-2})\right] \\ &\quad + \frac{F_N}{np\pi}\sum_{k=1}^{p}\left\{\mathrm{Sin}\left[n(p\alpha_{2k-1} - \pi)\right] - \mathrm{Sin}(np\alpha_{2k})\right\}.\end{aligned} \tag{17}$$

In (16) and (17), α_i is the error of the ith pole, see Fig. 6. For the effective component of the MMF,

$$\begin{aligned}f_{1s} &= \frac{F_P}{p\pi}\sum_{k=1}^{p}\left[\mathrm{Cos}(p\alpha_{2k-2}) + \mathrm{Cos}(p\alpha_{2k-1})\right] \\ &\quad + \frac{F_N}{p\pi}\sum_{k=1}^{p}\left[\mathrm{Cos}(p\alpha_{2k}) + \mathrm{Cos}(p\alpha_{2k-1})\right]\end{aligned} \tag{18}$$

$$\begin{aligned}f_{1c} &= \frac{F_P}{p\pi}\sum_{k=1}^{p}\left[\mathrm{Sin}(p\alpha_{2k-1}) - \mathrm{Sin}(p\alpha_{2k-2})\right] \\ &\quad + \frac{F_N}{p\pi}\sum_{k=1}^{p}\left[\mathrm{Sin}(p\alpha_{2k-1}) - \mathrm{Sin}(np\alpha_{2k})\right].\end{aligned} \tag{19}$$

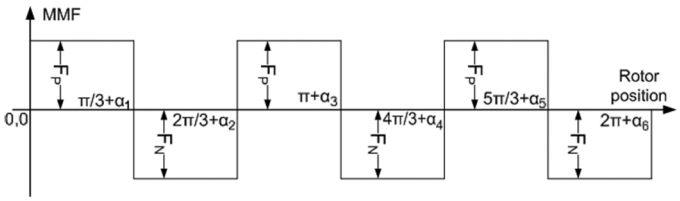

Fig. 6. The MMF of the PM ring in M1, and the pole-pitches contain errors.

As the pole-pitch error is normal very small, f_{ns} and f_{nc} shown from (16) to (19) can be expressed with the 1st order Taylor series as

$$f_{ns} = 0, \quad n > 1 \tag{20}$$

$$f_{nc} = \frac{F_P}{\pi p}\sum_{k=1}^{p}[(-1)^n\alpha_{2k-1} - \alpha_{2k-2}] + \frac{F_P}{\pi p}\sum_{k=1}^{p}[(-1)^n\alpha_{2k-1} - \alpha_{2k}] \tag{21}$$

$$f_{1s} = \frac{2}{\pi}(F_P + F_N). \tag{22}$$

Considering the continuous of the flux lines, and using the minimum energy method, the following result can be obtained:

$$F_P = K_a \cdot F_N \tag{23}$$

where

$$K_a = \left[\pi + \sum_{k=1}^{p}(\alpha_{2k} - \alpha_{2k-1})\right] \Big/ \left[\pi + \sum_{k=1}^{p}(\alpha_{2k-1} - \alpha_{2k-2})\right] \approx 1 + \frac{1}{\pi}\left[\sum_{k=1}^{p}(\alpha_{2k} - 2\alpha_{2k-1} + \alpha_{2k-2})\right]. \tag{24}$$

Therefore, (21) can be further expressed as

$$f_{nc} = \frac{F_N}{\pi p}\sum_{k=1}^{p}[(-1)^n 2\alpha_{2k-1} - \alpha_{2k-2} - \alpha_{2k}]. \tag{25}$$

From the point view of statistic analysis, it is clear, when p is increasing, K_a expressed by (24) should be more and more close to 1, f_{nc} of (25) will be more and more close to zero, and the effective MMF f_{1S} is more and more close to the one expressed by (7) That is, for the pole-pitch error in the same level, the influence of the error to the airgap magnetic field is weak. Therefore, increasing the pole-pair of the motor is very helpful in reducing the ZCP error.

Consider a special case. If only one pair of pole-pitches are not correct, e.g., the 1st pair, see Fig. 7. In this case, from (17), the following result can be obtained:

$$f_{nc} = \frac{(-1)^n \mathrm{Sin}(np\alpha_1)}{np\pi}(F_P + F_N). \tag{26}$$

The equation shows again that, increasing the magnetic pole-pair can reduce the influence of the pole-pitch error.

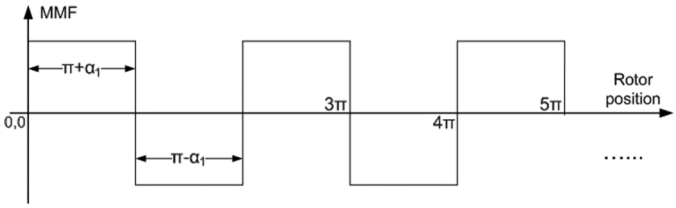

Fig. 7. Special case: only the 1st pair of pole-pitches contain errors (the unit of horizontal axis is electrical degree).

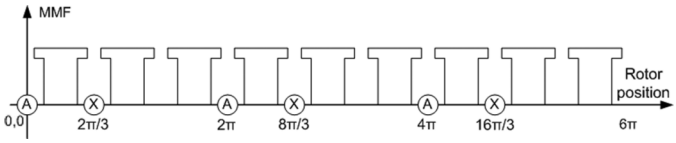

Fig. 8. The distribution of the A-phase winding in M1.

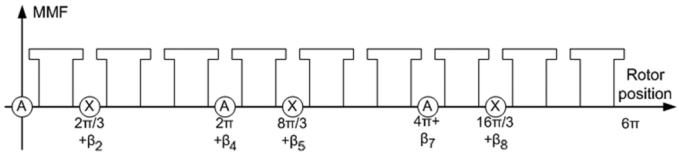

Fig. 9. M1: the A-phase winding distribution contains errors. (The horizontal axis is shown in electrical degrees.)

III. The Influence of the Stator Dimension Tolerance

The tolerance of the stator dimension can certainly affect the back-EMF generating, and induce error in the ZCP of back-EMF. For simplifying the analysis to the influence of the tolerance, in this section, it is assumed that the field produced by the PM ring is symmetric in the airgap.

It was mentioned in Section III that, all the spindle motors used in HDDs are using the concentrated fractional windings, as it is shown in Fig. 3. In order to make the analysis be clear, in this paper, the winding in one slot is assumed to be concentrated at the center point of the slot; see Fig. 8.

If the dimension tolerance of the slot is zero, all the teeth are symmetrically distributed in the space. The phase back-EMF induced in the winding can be expressed as the one shown in (10).

If there is dimension tolerance on the slot/tooth, the winding distribution is changed, as the ones shown in Fig. 9, and the back-EMF is changed to

$$e(t) = \sum_{k=1}^{p} e_{3k-2}(t) = -w\sum_{k=1}^{p}\frac{d\phi_{3k-2}(t)}{dt} = w\omega c_m \times \sum_{n=1}\left[\left[f_n \sum_{k=1}^{p}\left\{\mathrm{Sin}\left[(2n-1)\left(p\omega t + p\beta_{3k-2} - \frac{4\pi}{3}\right)\right] - \mathrm{Sin}\left[(2n-1)\left(p\omega t + p\beta_{3k-1} - \frac{2\pi}{3}\right)\right]\right\}\right]\right]. \tag{27}$$

If the tolerance β_k is small enough, (27) can be expressed as

$$e(t) = pw\omega c_m \sum_{n=1}\left[\left[f_n\left[\mathrm{Sin}\left[(2n-1)p\omega t\right] - \mathrm{Sin}[(2n-1)\left(p\omega t + \frac{2\pi}{3}\right)\right]\right]\right] + K_{cn} + K_{dn} \tag{28}$$

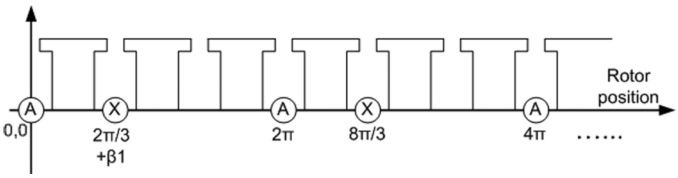

Fig. 10. A special case: only the 1st slot of the stator has position error. (The horizontal axis is shown in electrical degrees.)

where

$$K_{cn} = -\left(\sum_{k=1}^{p}\beta_{3k-1}\right) pw\omega c_m \times \sum_{n=1}\langle f_n \mathrm{Cos}\left[(2n-1)p\omega t\right]\rangle, \quad (29)$$

$$K_{dn} = -\left(\sum_{k=1}^{p}\beta_{3k-2}\right) pw\omega c_m \times \sum_{n=1}\left\langle f_n \mathrm{Cos}\left[(2n-1)\left(p\omega t+\frac{2\pi}{3}\right)\right]\right\rangle. \quad (30)$$

Comparing (28) with (10) it is clear, the existence of K_{cn} and K_{dn} tolerance make both the amplitude and phase angle of the phase back-EMF changed. This affects certainly the ZCP distribution in the three-phase system. However, as $pw\omega$ is constant, (29) and (30) show also that, from the point view of statistics, increasing p can reduce both K_{cn} and K_{dn}, i.e., weaken the influence of the tolerance to the ZCPs.

In the case that, only one stator slot is not in right position, e.g., the 2nd slot, see Fig. 10. In this case, from (27), the following result can be obtained from

$$K_e = -2pw\omega c_m \frac{\mathrm{Sin}\left[(2n-1)\frac{p\beta_2}{2}\right]}{p} \times \sum_{n=1}\left[\left[f_n\left[\left\{\mathrm{Cos}\left[(2n-1)\left(p\omega t+\frac{p\beta_2}{2}+\frac{\pi}{3}\right)\right]\right]\right]\right]. \quad (31)$$

The equation shows again that, in this case, as $pw\omega$ is constant, increasing the magnetic pole-pair can reduce K_b, and thus can weaken the influence of the dimension tolerance to ZCPs.

IV. The Influence of the Winding Turns

In the motor analysis, it is normally considered that the winding turns in all the stator slots are same. However, in the motor production, all the leading wires of the three-phase windings have to go through a hole together for simplifying the connector of the motor in linking with external drive circuit [6]. Therefore, for one phase winding, one, or two, slot could has more, or fewer, winding turns than its other slots, and the increased/reduced winding turn could be 0.5, or 1 [6]. From (10) the phase back-EMF can be written as

$$e(\omega t) = \frac{2pw\omega c_m F_A}{\pi} \times \sum_{n=1}\frac{\mathrm{Sin}\left[(2n-1)p\omega t\right] - \mathrm{Sin}\left[\frac{(2n-1)(2\pi+3p\omega t)}{3}\right]}{2n-1} \quad (32)$$

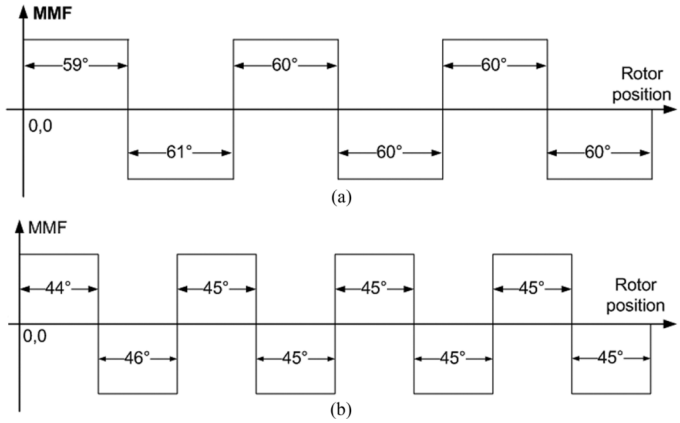

Fig. 11. Case-2: The pole-pitch error of PM ring is 1 degree (a) M1; (b) M2.

where c_m is related with motor airgap structure. Therefore, when the winding turn of one phase winding is changed, its back-EMF is also changed.

For a spindle motor, the value of pw is the total winding turns in one phase winding. From (32) for a given drive voltage and a speed, the product of $pw\omega$ should be constant for the spindle motor operating at same DC-Link voltage. For high speed motor, its total winding turns, pw, is quite low. Therefore, the back-EMF is quite sensitive to the winding turns. If windings of B and C phase are not affected by their leading wires, the leading wire of A phase will make three-phase back-EMFs be unbalanced. When the leading winding turn is 1, the following equation can be used to describe the three-phase back-EMF:

$$\begin{cases} e_a(t) = \left[1 \pm \frac{1}{pw}\right] E_m \mathrm{Sin}(\omega t+\varepsilon) \\ e_b(t) = E_m \mathrm{Sin}\left(\omega t+\varepsilon-\frac{2\pi}{3}\right) \\ e_c(t) = E_m \mathrm{Sin}\left(\omega t+\varepsilon-\frac{4\pi}{3}\right). \end{cases} \quad (33)$$

When the motor operates at constant speed, the unbalanced three-phase back-EMFs are asymmetric in the space time domain, and make the ZCP be distributed asymmetrically in the space domain. When using to calculate the motor speed, such a ZCP distribution will certainly produce speed error. (33) shows, the unbalance is serious to high speed spindle motor as its winding turns is few.

In Sections II and III, it was mentioned that, increasing magnetic pole-pair can reduce the ZCP errors induced by the pole-pitch error and slot dimension tolerance. But, from (32), this measure is not suitable to the error induced by the leading wires. Designing a reasonable winding to let the three-phase back-EMF be balanced is important in the spindle motor design.

V. Verifying the Influence of the EM Structure With Finite Element Analysis

For verifying the conclusions obtained in Sections II–V, several spindle motors have been analyzed with the finite element method (FEM) to investigate the influences of pole-pitch error, dimension tolerance and the leading wires of the spindle motor. Here, the results for two spindle motors, M1 and M2 are used for analysis. The materials used and dimensions of M1 and M2 are almost the same, the differences in these motors are their

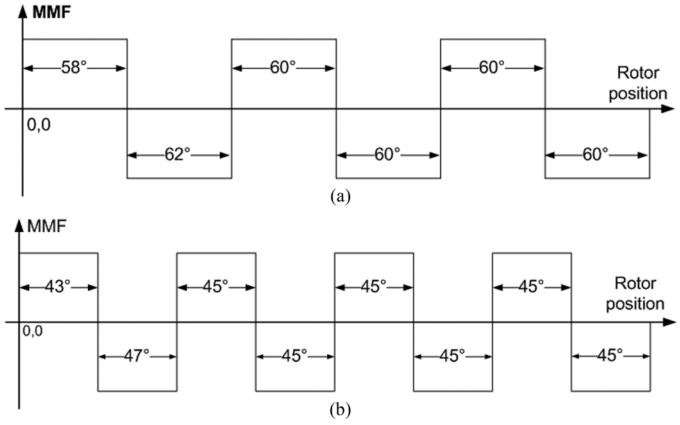

Fig. 12. Case-3: The pole-pitch error of PM ring is 2 degree. (a). M1; (b). M2.

TABLE I
THE ZCP INDUCED BY THE POLE-PITCH VARIATION

Pole-pitch error (Degree)	ZCP average absolute error of M1 (Degree)	ZCP average absolute error of M2 (Degree)
0	0.0007416	0.001313
1	0.3683	0.2182
2	0.6381	0.4343

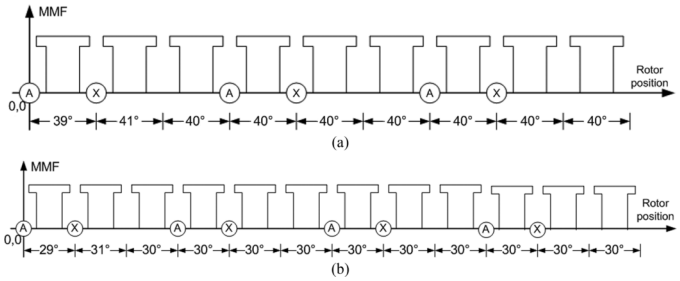

Fig. 13. Case-5: The error of one slot center is 1 degree. (a). M1; (b). M2.

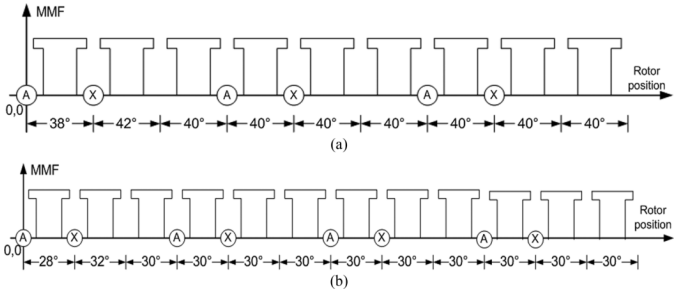

Fig. 14. Case-6: The error of one slot center is 2 degree. (a). M1; (b). M2.

pole-pair, slot number, and the dimensions related with stator slot.

Three cases of M1 and M2 were calculated for investigating the influence of the pole-pitch error to the ZCP error. In the Case-1, all the pole-pitches of the PM ring are correct. In the Case-2, only one pole-pitch was adjusted with 1 degree deviation; see Fig. 11. In the Case-3, the pole-pitch error is increased to 2 degree; see Fig. 12.

FEM is used to calculate the back-EMF of these motors, and the ZCPs were checked. The relative ZCP error calculated are

TABLE II
THE ZCP INDUCED BY THE SLOT DIMENSION TOLERANCE

Slot error (Degree)	Maximum ZCP error of M1 (Degree)	Maximum ZCP error of M2 (Degree)
1	0.1851	0.09553
2	0.3132	0.2144

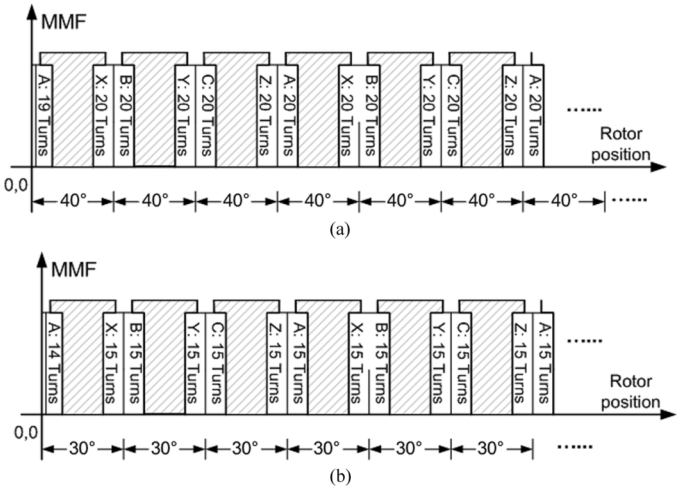

Fig. 15. Case-6: The winding turn in 1 slot is changed. (a) M1 (6 of 9 slots are displayed); (b) M2 (6 of 12 slots are displayed).

shown in Table I. In theory, the ZCP error in Case-1 is zero, and the error shown in the table is caused by the numerical method itself. From the Table, it can be found, as the magnetic pole-pair of M2 is more than M1, the influence of the pole-pitch error in M2 is weaker than M1. Therefore, the conclusions presented in Section III are confirmed in these cases.

Another 2 cases of M1 and M2 were calculated for investigating the influence of the slot tolerance to the ZCP error. In the Case-4, the center of one slot was deviated 1 degree from its center; see Fig. 13. In the Case-5, the center was deviated 2 degree from its center; see Fig. 14.

FEM is still used to calculate the back-EMF of these motors, and the ZCPs were checked. The calculated ZCP errors in these 2 cases are shown in Table II. From the Table, it can still be found, as the magnetic pole-pair of M2 is more than M1, its influence to the ZCPs is weaker than M1. Therefore, the conclusions presented in Section IV are confirmed in these cases.

The influence of leading wire is investigated with another two cases of M1 and M2. In the Case-6, all the slots have the same windings, only the winding turn in the 1st slot of A-phase winding is reduced with 1; see Fig. 15. In Case-7, the winding turns in both the 1st and 2nd slots of A-phase winding are reduced with 1; see Fig. 16. The influence of the leading wire is shown in Table III. The numerical results show that, in these 2 cases, the influence of the leading wire is almost same to M1 and M2, though the pole-pair of these two motors are different.

VI. CONCLUSION

The causes that induce error of the zero-crossing position are complicated, and parts of them are from the motor structure it-

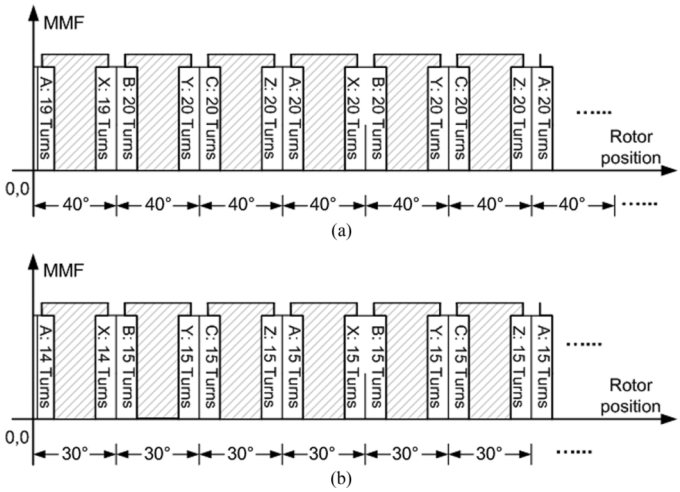

Fig. 16. Case-7: The winding turns in 2 slots are changed. (a) M1 (6 of 9 slots are displayed); (b) M2 (6 of 12 slots are displayed).

TABLE III
THE ZCP INDUCED BY THE LEADING WIRE

Turns of leading wire	ZCP average absolute error of M1 (Degree)	ZCP average absolute error of M2 (Degree)
0.5	0.04654	0.04592
1	0.1061	0.09232

self. These causes include the pole-pitch error of PM ring, the dimension tolerance of stator slot/tooth, and the leading wires of armature winding. All these error sources are induced during motor production.

The paper presents a method in using MMF to analyze the influences of these three reasons to the ZCP error. The analyzing results show that, from the point view of statistics, the influence of the pole-pitch error can be diminished in the spindle motor that possesses more magnetic pole-pairs. For the influence of the dimension tolerance of stator slot/tooth, using multiple magnetic pole-pair EM structure can also reduce the influence of the tolerance to the ZCP. For verifying the analytical results, one spindle motor with three magnetic pole-pair and one spindle motors with four magnetic pole-pairs are studied with FEM, and their ZCPs are examined. The numerical results confirm that the increasing the number of magnetic pole-pair can reduce the influence of pole-pitch error and dimension tolerance to the ZCP when the spindle motor is in operation.

However, the influence of the leading wires of the armature winding cannot be reduced by increasing the number of magnetic pole-pair. Designing reasonable leading wires to balance make the back-EMF of the three-phase windings is important in spindle motor design.

REFERENCES

[1] C. S. Soh, C. Bi, and K. K. Teo, "The FPGA implementation of quasi-BLDC drive," presented at the Seventh International Conference on Power Electronics and Drive Systems, Bangkok, Thailand, Nov. 27–30, 2007.

[2] C. S. Soh and C. Bi, "Self-sensing sinusoidal drive for spindle motor systems," in *IEEE IECON 2007*, Taipei, Taiwan, Nov. 5–8, 2007.

[3] S.-H. Lee, I.-H. Park, and K.-S. Lee, "Comparison of mechanical deformations due to different force distributions of two equivalent magnetization models," *IEEE Trans. Magn.*, vol. 34, no. 4, pp. 1368–1373, Jul. 2000.

[4] K. Miyata and K. Miya, "Magnetic field analysis of saturated steel," *IEEE Trans. Magn.*, vol. 34, no. 1, pp. 230–233, Jan. 1988.

[5] G. Reyne, G. Meunier, J. F. Imhoff, and E. Euxibie, "Magnetic forces and mechanical behavior of ferromagnetic materials. Presentation and results on the theoretical, experimental and numerical approaches," *IEEE Trans. Magn.*, vol. 24, no. 1, pp. 234–237, Jan. 1988.

[6] C. Bi, H. N. Phyu, and Q. Jiang, "Unbalanced magnetic pull induced by leading wires of permanent magnet synchronous motor," presented at the 12th International Conference on Electrical Machines and Systems (ICEMS 2009), Tokyo, Japan, Nov. 15–18, 2009.